Plant Communications
Research article

CellPress
Partner Journal

Cell specialization and coordination in *Arabidopsis* leaves upon pathogenic attack revealed by scRNA-seq

Etienne Delannoy[1,2], Bastien Batardiere[3], Stéphanie Pateyron[1,2], Ludivine Soubigou-Taconnat[1,2], Julien Chiquet[3], Jean Colcombet[1,2] and Julien Lang[1,2,*]

[1]Université Paris-Saclay, CNRS, INRAE, Université Evry, Institute of Plant Sciences Paris-Saclay (IPS2), 91190 Gif sur Yvette, France

[2]Université Paris Cité, CNRS, INRAE, Institute of Plant Sciences Paris-Saclay (IPS2), 91190 Gif sur Yvette, France

[3]UMR MIA Paris-Saclay, Université Paris-Saclay, AgroParisTech, INRAE, 91120 Palaiseau, France

***Correspondence: Julien Lang (julien.lang@inrae.fr)**

https://doi.org/10.1016/j.xplc.2023.100676

ABSTRACT

Plant defense responses involve several biological processes that allow plants to fight against pathogenic attacks. How these different processes are orchestrated within organs and depend on specific cell types is poorly known. Here, using single-cell RNA sequencing (scRNA-seq) technology on three independent biological replicates, we identified several cell populations representing the core transcriptional responses of wild-type *Arabidopsis* leaves inoculated with the bacterial pathogen *Pseudomonas syringae* DC3000. Among these populations, we retrieved major cell types of the leaves (mesophyll, guard, epidermal, companion, and vascular S cells) with which we could associate characteristic transcriptional reprogramming and regulators, thereby specifying different cell-type responses to the pathogen. Further analyses of transcriptional dynamics, on the basis of inference of cell trajectories, indicated that the different cell types, in addition to their characteristic defense responses, can also share similar modules of gene reprogramming, uncovering a ubiquitous antagonism between immune and susceptible processes. Moreover, it appears that the defense responses of vascular S cells, epidermal cells, and mesophyll cells can evolve along two separate paths, one converging toward an identical cell fate, characterized mostly by lignification and detoxification functions. As this divergence does not correspond to the differentiation between immune and susceptible cells, we speculate that this might reflect the discrimination between cell-autonomous and non-cell-autonomous responses. Altogether our data provide an upgraded framework to describe, explore, and explain the specialization and the coordination of plant cell responses upon pathogenic challenge.

Key words: scRNA-seq, plant defense responses, plant immunity, plant susceptibility, *Arabidopsis*/*Pseudomonas* interactions, biotic stress

Delannoy E., Batardiere B., Pateyron S., Soubigou-Taconnat L., Chiquet J., Colcombet J., and Lang J. (2023). Cell specialization and coordination in *Arabidopsis* leaves upon pathogenic attack revealed by scRNA-seq. Plant Comm. **4**, 100676.

INTRODUCTION

In presence of pathogens, plant responses are characterized by a combination of immune and susceptible processes whose balance ultimately determines the degree of plant resistance. Plant immunity is traditionally described as a two-layered system relying on two distinct perception machineries (Jones and Dangl, 2006). In the first one, conserved pathogen-associated molecular patterns (PAMPs) are recognized by surface-localized pattern-recognition receptors (PRRs), resulting in PAMP-triggered immunity (PTI). In the second layer, effectors that are secreted by the pathogens in the plant cells are recognized by cytoplasmic nucleotide-binding leucine-rich receptors (NLRs) leading to effector-triggered immunity (ETI). The arsenal of PRRs and NLRs are particularly rich in plants and allow them to mount effective defense responses against a large scope of pathogens with different trophic lifestyles (Zipfel, 2014; Jones

Published by the Plant Communications Shanghai Editorial Office in association with Cell Press, an imprint of Elsevier Inc., on behalf of CSPB and CEMPS, CAS.

et al., 2016; Ngou et al., 2022). Recent advances also showed that PTI and ETI do not necessarily constitute independent types of immunity but can be interconnected at different nodes, reciprocally potentiating each other. Thus, PTI is needed for fully efficient ETI caused by various effectors, while ETI promotes the expression of key PTI actors (Ngou et al., 2021; Yuan et al., 2021). Consistently PTI and ETI appear to converge toward a comparable gene reprogramming that is constantly fine-tuned or modified by the emergence and imbrication of new signaling such as the ones mediated by the hormones salicylic acid (SA), jasmonates (JA), ethylene (Et), and abscisic acid (ABA) (de Torres-Zabala et al., 2007; Zhang et al., 2018; Lu and Tsuda, 2020; Zhang and Fan, 2020). In parallel, plant susceptibility is generally understood as the outcome of impaired immune responses, usually because of the action of unrecognized pathogen effectors able to counteract and sabotage key immune actors. In this case we talk of effector-triggered susceptibility (ETS) (Jones and Dangl, 2006).

Although PTI, ETI, and ETS provide a powerful framework to explain plant defense responses, the temporal and spatial dimensions through which they exert their actions remain poorly characterized. Indeed, plant organs are composed of different tissues and cell types which therefore might respond differently to pathogen presence and give rise consequently to specific cell-type immunity or susceptibility. Moreover, pathogen colonization is a dynamic process that starts at specific entry points and then spreads throughout the host organs along possibly preferential paths, depending on how the various plant cell types can integrate this progression (Yu et al., 2013). Also, communication between cells that are directly sensing pathogens and cells that are still safe might stimulate, even within a population of the same cell type, two different kinds of responses (cell-autonomous responses for those in direct contact with the pathogens and non-cell-autonomous for the others) (Emonet et al., 2021). Till recently these questions could not be directly addressed because of technical limitations. Nonetheless cell-type immunity is a well admitted concept in the field. For instance, it is common to mention stomatal immunity as a guard cell-specific defense process preventing pathogens to penetrate tissues and colonize plant apoplast, even if the underlying molecular mechanisms are not totally elucidated so far (Melotto et al., 2017). In line with this, a recent study focusing on *Arabidopsis* root epidermis, cortex, and pericycle cells, also showed that PTI responses are driven mostly by cell identity, a finding that reinforces the validity of cell-type immunity (Rich-Griffin et al., 2020b). Yet a comprehensive understanding of how the complex heterogeneity of cell types might affect defense response is still lacking, and in this regard, newly-developed single cell technologies constitute unprecedented tools to undertake such investigations (Rich-Griffin et al., 2020a).

The bacterial *Pseudomonas syringae* pv. *tomato* DC3000 (*Pst*) strain is routinely used as a model hemibiotrophic pathogen of the plant phyllosphere. Its virulence is mediated by 32 effectors that are injected in the plant host through a type III secretory system. Among those, 8 are of special importance to promote colonization, notably by creating an aqueous apoplast environment (Xin et al., 2018; Hu et al., 2022). In addition, *Pst* produces the toxin coronatine, a JA mimic, that antagonizes SA defense pathways, and stomatal closure (Geng et al., 2012; Toum et al., 2016). The presence of *Pst* in the plant leaves leads to what is termed basal resistance or basal immunity, i.e., a combination of PTI, ETI, and susceptibility due to the effects of *Pst* virulence factors. In the literature we can find the description of several actors and processes that support basal immunity, including hormone signaling (Flors et al., 2008), kinase signaling (Shubchynskyy et al., 2017), reactive oxygen species (ROS) production (Velásquez et al., 2017), response to hypoxia (Hsu et al., 2013), response to unfolded protein (Nekrasov et al., 2009; Jelenska et al., 2010), lignification (Lee et al., 2019) or production of defensive secondary metabolites such as camalexin (Qiu et al., 2008) and glucosinolates (Fan et al., 2011). Different time course transcriptional analyses of plant leaves challenged with *Pst* are also available, offering a dynamic view of basal immunity (Lewis et al., 2015; Mine et al., 2018). However, all these studies were performed on bulk samples and therefore do not allow to determine whether the described defense responses take place in particular cell populations.

Here, using single-cell RNA sequencing (scRNA-seq) technology, on *Arabidopsis* leaf cells inoculated with *Pst*, we could reveal distinct cell classes, characterized by both specific and common defense transcriptional dynamics, thereby unveiling a new and original map of the battlefield between plants and pathogens.

RESULTS

scRNA-seq analysis reveals several biologically relevant cell populations in *Arabidopsis* leaves challenged with *Pst*

To investigate cell-type defense responses, we spray-inoculated *Arabidopsis* plants with a low-concentrated solution of *Pst* and collected the leaves 16 h later. At this time point, we observed a restrained colonization of the plant tissues by the pathogens, mainly in the ostioles and the apoplast of the mesophyll (Supplemental Figure 1), suggesting that a large portion of the plant cells should remain unaffected by the pathogens, and could be used as a healthy control to decipher the single-cell responses to *Pst*. Leaf protoplasts were produced using a short digestion protocol to minimize the protoplasting effects on transcriptomes, and were processed through the microfluidic Chromium technology (10X Genomics) to generate scRNA-seq libraries. We repeated this experimental procedure three independent times and obtained three independent dataset we pooled by concatenation. The cell clustering was carried out on the pooled dataset and resulted in the identification of 18 distinct cell populations (C0–C17) including 11 206 high-quality cells. The median numbers of genes and reads per cell are 2386 and 7676, respectively. The uniform manifold approximation and projection (UMAP) of the 18 clusters is shown in Figure 1A. The numbers of cells in each cluster range from 1003 for the largest cluster (C0) to 61 for the smallest cluster (C17) (Supplemental Table 1).

To understand the biological relevance of the 18 cell populations, we first analyzed the expression levels, in the different cells of the different clusters, of various cell-type marker genes found in the literature. These genes included markers of mesophyll cells, epidermal cells, guard cells, companion cells, vascular S cells and hydathode cells (Kim et al., 2021; Routaboul et al., 2022;

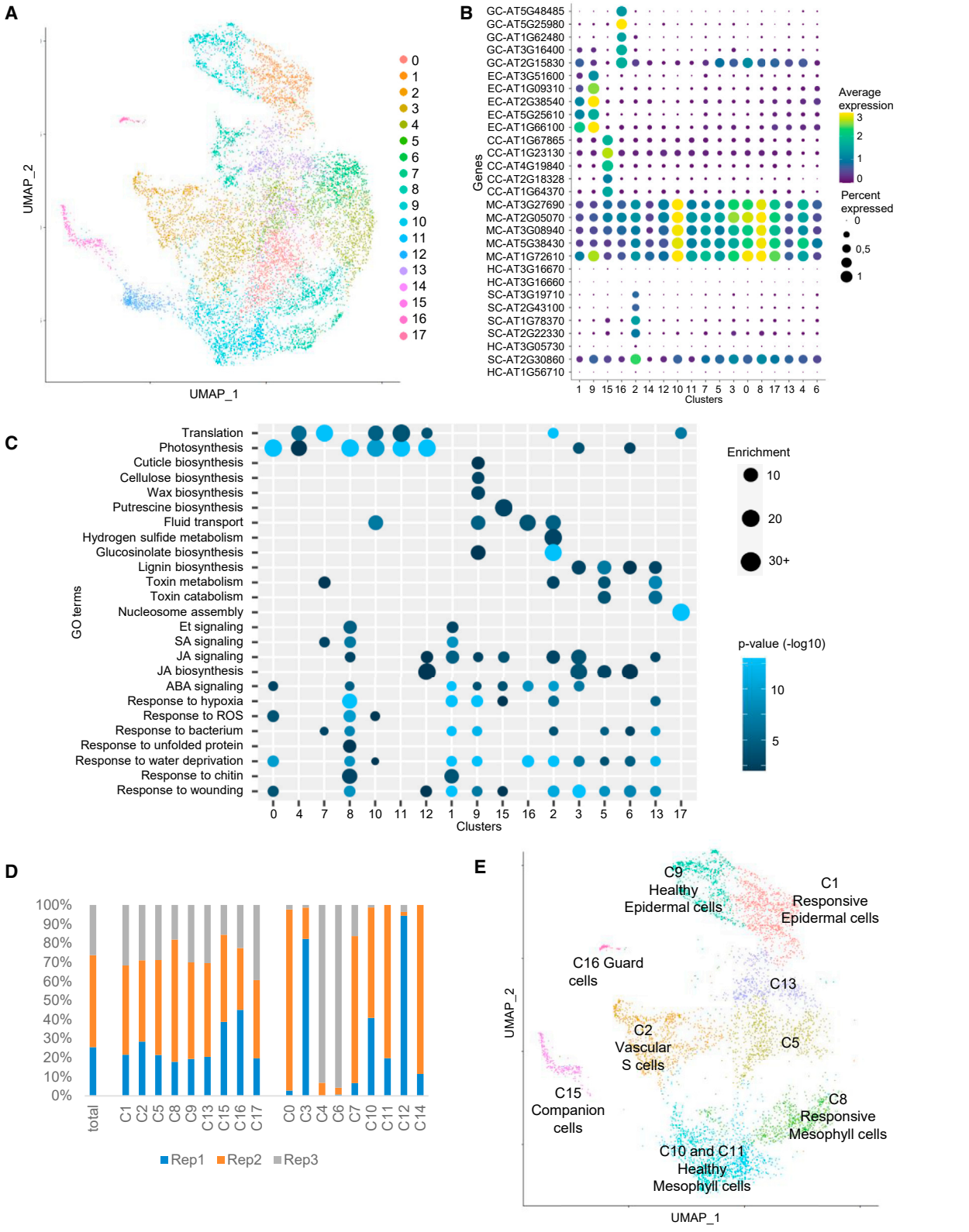

Figure 1. Identification of several biologically relevant leaf cell populations in response to *Pst*.

(A) UMAP projection of the 18 clusters obtained using principal-component analysis (see methods).

(B) Cluster-specific expression profiles of cell-type marker genes. The marker genes were selected from the literature (Kim et al., 2021; Routaboul et al., 2022; Tenorio Berrío et al., 2022). GC, CC, EC, HC, MC, and SC stand for guard cells, companion cells, epidermal cells, hydathode cells, mesophyll cells, and vascular S cells, respectively.

(legend continued on next page)

Tenorio Berrío et al., 2022). Remarkably this method allowed us to identify in a relatively straightforward manner the cell identities of 11 clusters (Figure 1B). C0, C3, C4, C8, C10, and C17 are thus a priori mesophyll cells, C9 and C1 are a priori epidermal cells, while C2, C15, and C16 correspond a priori to vascular S cells, companion cells, and guard cells, respectively. Even if they show high expression levels of mesophyll marker genes, the identities of C5, C6, C7, C11, C12, C13, and C14 remained at this step uncertain. No cluster could be attributed to the hydathode identity, maybe because our experimental conditions did not permit the recovery of such cell type.

Next, we created a list of upregulated marker genes for each cluster (Supplemental Table 2). This list displays several hundred of marker genes for all clusters, except C14 which displays only 43 marker genes. We therefore considered C14 as a clustering artifact and removed it from subsequent investigation. Using the list of marker genes we performed Gene Ontology (GO) analysis, and revealed in the different clusters specific enrichments in biological processes related to stress responses and to cell identity (Figure 1C; Supplemental Table 2). Consistently with their mesophyll annotation, C0, C4, C8, and C10 show the strongest enrichments in processes related to photosynthesis and translational elongation. Similarly, C7, C11, and C12 show strong and specific enrichments in these processes, supporting the notion that those clusters are also mesophyll cells. Besides, C7, C8, and C12 show enrichments in processes such as Et, SA, and JA signaling pathways, responses to hypoxia and ROS, or response to bacterium, suggesting that these three clusters correspond to responsive mesophyll cells, whereas C0, C4, C10, and C11 correspond to healthy mesophyll cells. The C8 notably shows a specific enrichment in response to unfolded protein. The epidermal C9 is characterized by fluid transport, cuticle development, and wax and cellulose biosynthetic processes, while C1 shows enrichments in processes related to responses to chitin, hypoxia, JA/SA/Et/ABA-signaling pathways, suggesting that C9 and C1 correspond to healthy and responsive epidermal cells, respectively. The companion cell C15 shows a strong enrichment in polyamine synthesis, especially in putrescine synthesis, an observation that can be related to the role of polyamines in biotic stress responses and their apparent privileged transport through phloem tissues (Friedman et al., 1986; Jiménez-Bremont et al., 2014). C16, identified as the cluster of guard cells, appears to be driven mostly by ABA-related processes, which is congruent with the well-established role of ABA in the regulation of stomata aperture and water transport (Bharath et al., 2021). C2 shows specific and strong enrichments in hydrogen sulfide metabolism and glucosinolate biosynthetic processes, confirming that C2 should encompass the vascular S cells of the phloem parenchyma in which glucosinolate biosynthesis typically occurs (Nintemann et al., 2018). In addition, our GO analysis found that four clusters were characterized only by processes related to stress responses. Thus C3, C5, C6, and C13 show strong enrichments in JA signaling, lignification, and detoxification. At last, C17 includes preponderantly GO terms associated with nucleosome assembly and chromatin remodeling, suggesting that cells of this cluster could undergo division or endoreplication. In parallel, we evaluated the transcriptional effects of protoplasting by looking at wounding responses which are also indicative of protoplasting responses (Figure 1C). Interestingly we did not observe strong or global enrichments in this process and it did not impair the characterization of specific responses to biotic stress, strongly indicating that protoplast generation had only weak impact on cell transcriptomes.

To further rationalize our clustering, we looked at the cell distribution between the three biological replicates in each cluster. As shown in Figure 1D, we detected drastic replicate bias for some clusters, unveiling important variations between the three independent inoculations, as it might be expected in the study of complex interactions between plant and microbes. Nonetheless, C1, C2, C5, C8, C9, C13, C15, C16, and C17 exhibit a cell distribution between the three replicates that is in line with the distribution in the total number of cells. We therefore inferred that these 9 clusters contain the most robust biological information and epitomize the plant transcriptional responses to the pathogen. Remarkably we retrieved among them all the cell types we identified previously through the marker approach and the GO analysis, with the notable exception yet of the healthy mesophyll cells. Indeed, C10 and C11 appear to be specific of replicates 1 and 2, whereas C0 and C4 are composed almost uniquely of cells coming from replicates 1 and 3, respectively (Figure 1D; Supplemental Figure 2). As leaves from the three replicates were exposed to slightly different light periods before harvest (see methods), an explanation could be that scRNA-seq is powerful enough to capture differences in the photosynthesis program between the three biological repetitions. Alternatives could be differences in the circadian rhythm or clustering artifacts. Either way, the marker genes of these four clusters largely overlap (Supplemental Table 2), clearly indicating that they encompass very close populations.

Taken altogether our preliminary analyses came to the identification of several biologically relevant cell clusters (Figure 1E). To further characterize the defense responses of these clusters, we focused on the most strongly and significantly upregulated genes (fold change [FCh] $\geq 2^{0.7}$, adjusted $p < 0.05$) (Supplemental Table 3). In the following, marker genes will always refer to this more stringent definition, unless otherwise mentioned.

Characteristic epidermal defense response

To characterize epidermal defense responses, we first compared C9 marker genes with a list of epidermal genes coming from an

(C) Enrichments in biological processes for marker genes in each cluster and associated p values were generated using Panther. For a complete list of GO enrichments, see Supplemental Table 2.

(D) Cell repartition between the three biological replicates in the total population and in each cluster. Among the total 11 206 cells of the analysis, 2861 (25,5%) come from replicate 1 (Rep1), 5397 (48%) from replicate 2 (Rep2), and 2948 (26,5%) from replicate 3 (Rep3).

(E) UMAP projection of the relevant clusters. Annotation was performed from expression profiles of cell-type marker genes and GO analysis. For simplification, only C10 and C11 are shown as representative of healthy mesophyll cells.

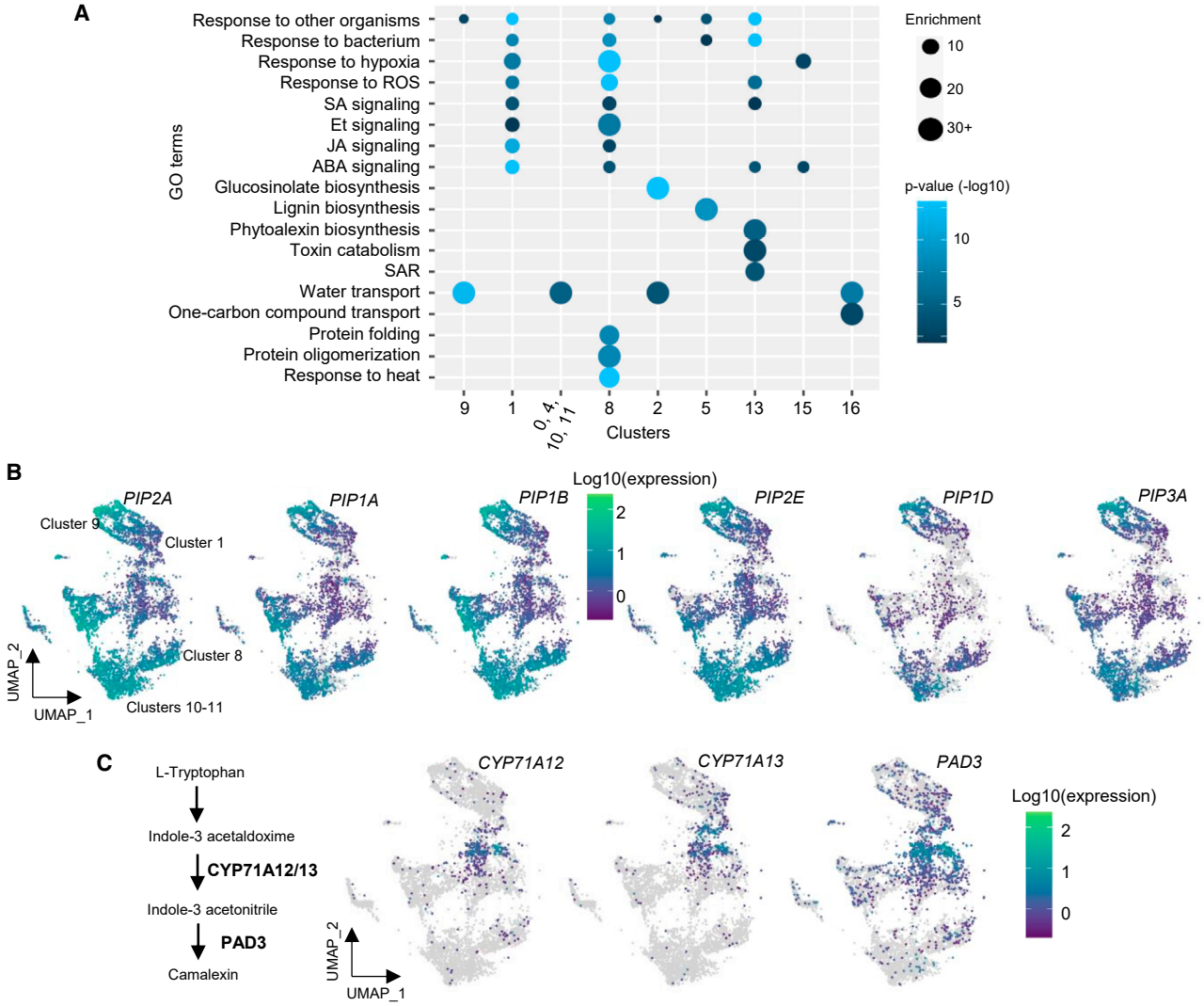

Figure 2. Cell-type-characteristic responses to *Pst*.

(A) Enrichments in biological processes for stringent marker genes in each of the selected clusters and associated p values were generated using Panther. For complete lists of GO enrichments, see Supplemental Table 3.

(B) Cell-specific expression profiles of 6 aquaporin genes in the UMAP projection.

(C) Cell-specific expression profiles of genes involved in camalexin synthesis in the UMAP projection. Schematic description of the biosynthetic pathway of camalexin is shown on the left.

independent scRNA-seq experiment performed on non-challenged *Arabidopsis* plants of the same age (Kim et al., 2021). We observed a strong overlap between the two sets of genes (64/130 for C9) (Supplemental Table 3), confirming again the healthy epidermal identity of the C9 cells. Nonetheless, among the genes which are specific to C9 compared with Kim et al., we found enrichments for processes related to water transport and response to other organisms (Figure 2A). Six plasma membrane-intrinsic protein (PIP) aquaporin genes are thus part of the C9 marker genes: *PIP2E*, *PIP1A*, *PIP1D*, *PIP1B*, *PIP3A*, and *PIP2A*. This is consistent with the notion that water allocation is a critical process at the interface between the host and the pathogen (Xin et al., 2016). Regarding genes associated with response to other organisms, we noticed that several of them are involved in Et synthesis and signaling, such as the *ACC synthase 6* and the *ACC oxidase 2* genes, as well as five Et response factors: *ERF017*, *ERF5*, *ERF109*, *ERF018*, and *ERF72*. In addition, we found among the C9 markers several genes encoding proteins involved in biotic stress response. Those include *AT2G45180*, a nsLTP family-related gene whose expression was recently reported to be suppressed by *Pst* (Dhar et al., 2020), *AT4G14450* encoding a proline/serine rich protein that interacts with the immune kinase MPK6 and whose expression is induced by PAMPs (Palm-Forster et al., 2017), and *RALF23*, and *PREPIP1*, which code for small peptides acting as phytocytokines (Hou et al., 2014; Stegmann et al., 2017). Interestingly, when we plotted the expression levels of all these 17 genes in the UMAP representation, we observed that they progressively decreased between cells from C9 and C1 populations (Figure 2B; Supplemental Figure 3), indicating that these genes are very likely repressed in response to *Pst*.

The C1 cluster that we identified as the responsive epidermal cluster also shares numerous marker genes with the set of healthy epidermal genes from Kim et al. (2021) (48/151), (Supplemental Table 3). C1 and C9 have 12 marker genes in common, 8 of them appearing to be epidermal markers according to Kim et al. (2021), the 4 others being *AT1G25275*, a thionin-like gene, *AT1G66090* a TIR-NBS gene upregulated during PTI and ETI (Lang et al., 2022), *AT2G05520* an ABA-, SA-, and Et-responsive gene encoding a glycine-rich protein, and the E3 ligase *AT4G17245*. The expression profiles of these 4 genes showed that they either progressively increase between cells from C9 and C1 populations or remain at the same levels (Supplemental Figure 4), suggesting either that their induction mediate early epidermal responses to the pathogen or that they are new markers of the epidermal cells. In the specific C1 marker genes (compared with Kim et al., 2021), we retrieve many stress genes that overall depict a response to *Pst* characterized mainly by hypoxic and ROS stresses as well as by hormone signaling (JA, ABA, and SA) (Figure 2A; Supplemental Table 3). Remarkably, using TF2Network (Kulkarni et al., 2018) to search for transcriptional regulators that may explain the expressions of the C1 marker genes, we found that the most important transcriptional factors are WRKY transcription factors (Supplemental Table 4). In contrast no consistent list of transcriptional regulators could be generated for C9.

Taken collectively the data from C1 and C9 delineate an epidermal transcriptional reprogramming upon *Pst* infection characterized mainly, on one hand, by the inhibition of water transport and of some Et signaling components and, on the other hand, by the activation of WRKY-guided responses to ROS, hypoxia, JA, SA, and ABA.

Characteristic guard cell defense response

By comparing the 58 marker genes of C16 with the list of unchallenged guard cell marker genes from Kim et al. (2021), we found an overlap of 12 members, notably among the highest expressed genes (Supplemental Table 3), which comforted us in the attribution of guard cell identity to C16. Specific C16 marker genes compared with Kim et al. (2021) revealed important GO enrichments in processes such as transport of fluid/water (involving the aquaporin genes *PIP2A*, *PIP1B*, and *PIP2B*), transport of one-carbon compounds (such as CO_2) as well as response to desiccation (Figure 2A; Supplemental Table 3). These data suggest that ABA plays an important role in the adaptation of C16 cells to *Pst*. Consistently, analysis with TF2Network proposes the ABA responsive elements-binding factors 2 and three other bZIP transcription factors as the most important regulators for C16 reprogramming (Supplemental Table 4). Furthermore, if in the guard cell data from Kim et al. (2021), the myrosinase *TGG1* is not detected while *TGG2* is the strongest upregulated gene, in our data, among the C16 marker genes, both *TGG1* and *TGG2* are the two genes with the highest upregulation levels (Supplemental Table 3), suggesting that *TGG1* induction could be a specific response to *Pst*.

Overall C16 tends to show that guard cell responses to *Pst* are mostly governed by ABA signaling. This is consistent with the known role of ABA in the positive regulation of stomata closure, limiting the ability of the pathogen to colonize the plant host (Bharath et al., 2021). In addition, guard cells could also contribute to the mustard-oil bomb strategy of defense against *Pst* through the expressions of the myrosinases *TGG1* and *TGG2* which are known to be involved in the production of toxic glucosinolate-derived compounds preventing massive invasion of the pathogen (Barth and Jander, 2006; Zhang et al., 2019).

Characteristic mesophyll defense response

Our preliminary analyses allowed identifying C0, C4, C10, and C11 as encompassing healthy mesophyll cells. In line with this, there is a strong overlap between the marker genes of these four clusters and the mesophyll marker genes of unchallenged plants from the study of Kim et al. (2021) (187/240) (Supplemental Table 3). Moreover the 53 remaining specific marker genes of C0, C4, C10, and C11 are predominantly annotated as involved in photosynthetic process, albeit we retrieved among them enrichments in water transport processes with notably the genes *PIP2A*, *PIP1A*, *PIP1B*, and *PIP2E*. Again, this observation indicates that repression of aquaporin genes might represent an important response to *Pst* as it was already observed in epidermal cells (Figure 2B).

In contrast to C0, C4, C10, and C11, C8 seems to correspond to the responsive mesophyll cluster. Thirty of the 101 C8 marker genes are mesophyll marker genes according to Kim et al. (2021). As for the other 71 marker genes, they are mostly stress related and globally uncover a basal defense response to *Pst* that is somehow reminiscent of the epidermal C1, i.e., characterized by responses to hypoxic and oxidative stress as well as hormone signaling (JA, SA, Et, and ABA) (Figure 2A; Supplemental Table 3). Yet responsive epidermal (C1) and C8 marker genes have no members in common, hinting at some decisive differences between the two kinds of responses. For instance, several Et actors that are repressed in C1 responsive epidermal cells are induced in C8 responsive mesophyll cells (Supplemental Figure 3). Similarly the kinase *MKK9* that is an important actor for Et synthesis and for transduction of Et effects is a specific marker of C8 (Supplemental Table 3) (Xu et al., 2008; Yoo et al., 2008). Besides, C8 displays specific enrichment in processes related to protein folding, protein oligomerization, and response to heat stress, with several heat shock proteins, especially small heat shock proteins, among the most strongly expressed marker genes (*HSP17.6A*, *HSP17.6B*, *HSP17.6C*, *HSP17.6II*, *HSP17.4*, *HSP17.4B*, *HSP17.8*, *HSP70B*, *HSP70-4*, *HSP81-2*, and *HSP101*) as well as the heat shock factor *HSFA2* (Figure 2A; Supplemental Table 3). Additionally, a search of TF2Network revealed that the most important transcriptional regulators for C8 are CAMTA1/2/3, HSFA1E and HSFA6A/B (Supplemental Table 4).

Altogether it seems that mesophyll responses to *Pst* resemble those of epidermal cells, with, for instance, the downregulation of several aquaporin genes (Figure 2B) and the enrichments in GO functions related to stress responses that greatly overlap between the two cell types (Figure 2A; Supplemental Table 3). However, a deeper look at the marker genes and their transcriptional regulators reveals important differences in the molecular mechanisms that underpin their respective responses. Notably, Et signaling seems preponderant in

responsive mesophyll cells compared with responsive epidermal cells, and also, whereas characteristic epidermal reprogramming is WRKY mediated, characteristic mesophyll reprogramming involves predominantly CAMTAs and HSFs.

Characteristic vascular defense responses

Leaf vasculatures are complex tissues encompassing several cell types (Kim et al., 2021). In our data, we identified only two types of vascular cells: the companion cells (C15) and the vascular S cells (C2), likely because our protocol for protoplast production does not allow us to recover other cell types. However, another possibility we cannot totally rule out is that our two vasculature populations are actually a composite of several other cell subtypes.

Among the 127 marker genes of C15, 63 are common with the marker genes of companion cells from healthy leaves (Kim et al., 2021), while the 64 others depict a stress response driven mostly by hypoxia and ABA signaling (Figure 2A; Supplemental Table 3). In those latter 64 genes, the most strongly expressed ones are two metallothionein (MT3 and MT2B), a thioredoxin (TRX3), two cyclophilins (ROC1 and ROC5), and a dehydrin (HIRD11), suggesting that companion cells could also respond to *Pst* through the implementation of protective measures against ROS (Supplemental Table 3).

Interestingly the vascular S cells were not found in the study of Kim et al. (2021), raising the hypothesis that C2 cluster could be a hallmark of induced responses to *Pst*. C2 marker genes show strong enrichments in metabolism of aliphatic glucosinolates with notably the cytochrome P450 *CYP83A1* or the glucosinolate transporter *GTR1* (Figure 2A; Supplemental Table 3). This indicates that vascular S cells could mostly contribute to defense responses to *Pst* through the mustard-oil bomb strategy, likely in collaboration with the guard cells that exhibit high expression levels for myrosinases.

C5 and C13 are related stress-specific cell populations

In our clustering we identified two cell populations to which we could not assign any cell identity but that are characterized by strong stress responses. C5 shows important enrichments in the lignification process as well as in response to biotic stress such as bacterium (Figure 2A; Supplemental Table 3). For instance, we found in the C5 marker genes, *CASPL4D2* and *CASPL1D1*, corroborating the recent literature showing that these two genes encode two essential enzymes for the organization of lignin polymers in response to *Pst* (Lee et al., 2019). The C5 marker genes also include several genes known to be induced upon pathogenic bacterial challenge such as *AT3G22600*, *AT4G22470*, or *AT4G37990* (Supplemental Table 3).

The C13 population is characterized mainly by phytoalexin synthesis, detoxification, and SA-mediated defense responses, especially SAR (Figure 2A; Supplemental Table 3). For instance, *PAD3* and *CYP71A12/13* are strongly expressed in C13, indicating that camalexin production is likely specific to this cluster (Figure 2C). Such compartmentalization in a specific cell population of key transcriptionally-regulated immune pathways has also been established in another recent study (Nobori et al., 2023). In addition, several glutathione-S transferases, metal transporters or secretory carriers, endochitinases, or NDR1-like genes are upregulated in C13. Interestingly we found 4 *WRKY* transcription factors among the C13 marker genes (*WRKY8*, *WRKY29*, *WRKY55*, and *WRKY75*), suggesting that these regulators play critical roles for the reprogramming of C13 (Supplemental Table 3).

We also noticed that, in line with their contiguity in the UMAP projection, C5 and C13 have 12 marker genes in common, including *CASPL4D2* and *CASPL1D1* (Supplemental Table 3). This suggests that the two cell populations are actually close in terms of transcriptional reprogramming. Consistently similar WRKY and ANAC transcription factors appear to control the expression of the marker genes in C5 and C13 (Supplemental Table 4). Taken altogether our data indicate that C5 and C13 might form a continuum of response to *Pst*, characterized mostly by WRKY-mediated immune processes such as the production of phytoalexins and lignin that can act as barriers against the propagation of the pathogen (Qiu et al., 2008; Lee et al., 2019). They also highlight the fact that defense responses can lead to profound modifications, both up and down, of various transcript levels that can eventually alter cell identity in a substantial manner.

Inequalities in pathogen sensing between cell populations

As we identified characteristic transcriptional reprogramming in different cell types, we were prompted to see whether these differences could be correlated with differences in the ability to sense the pathogens between the cell types. To address this question, we focused on the expression profiles of the *NLR* gene family as well as on those of the leucine-rich repeat (LRR) and LysM-containing gene classes of the *PRR* family (Shiu and Bleecker, 2001; Meyers et al., 2003). As shown in Figure 3, Supplemental Figures 5 and 6, our data unveiled important differences in the expression levels of the immune receptors between the different cell populations. First, we observed that overall, both the number of expressed receptors and their expression levels increase in the responsive clusters C1, C5, C8, and C13 compared with the non-responsive clusters C9, C10, and C11. Importantly we retrieve among the immune receptors that are the most strongly expressed, genes that are well known to be involved in defense responses to *Pst*, such as the PRRs *FLS2*, *EFR*, *BAK1*, and *LYK1* or the NLRs *ZAR1*, *SNC1*, and *NRG1.1*. In parallel we observed that the expression levels of the immune receptors remain globally moderate in the C2 vascular S cells, the C15 companion cells and the C16 guard cells, suggesting that these cell types might, to some significant degree, respond to *Pst* through other receptor machineries. However, it must also be noted that for these cell types we could not separate healthy and responsive populations, hence it is possible that the percentage of cells expressing immune receptors as well as their expression levels remain underestimated in these clusters compared with the responsive C1, C5, C8, and C13. At last, it is worth noting that in the healthy epidermal cells (C9), both PRRs and NLRs are more expressed than in healthy mesophyll cells (C10 and C11), suggesting that the two cell types are unequal in their ability to sense the pathogens. Moreover, if the PRRs are the most numerous to be strongly induced in the responsive epidermal cells (C1) as well as in the C5 and C13

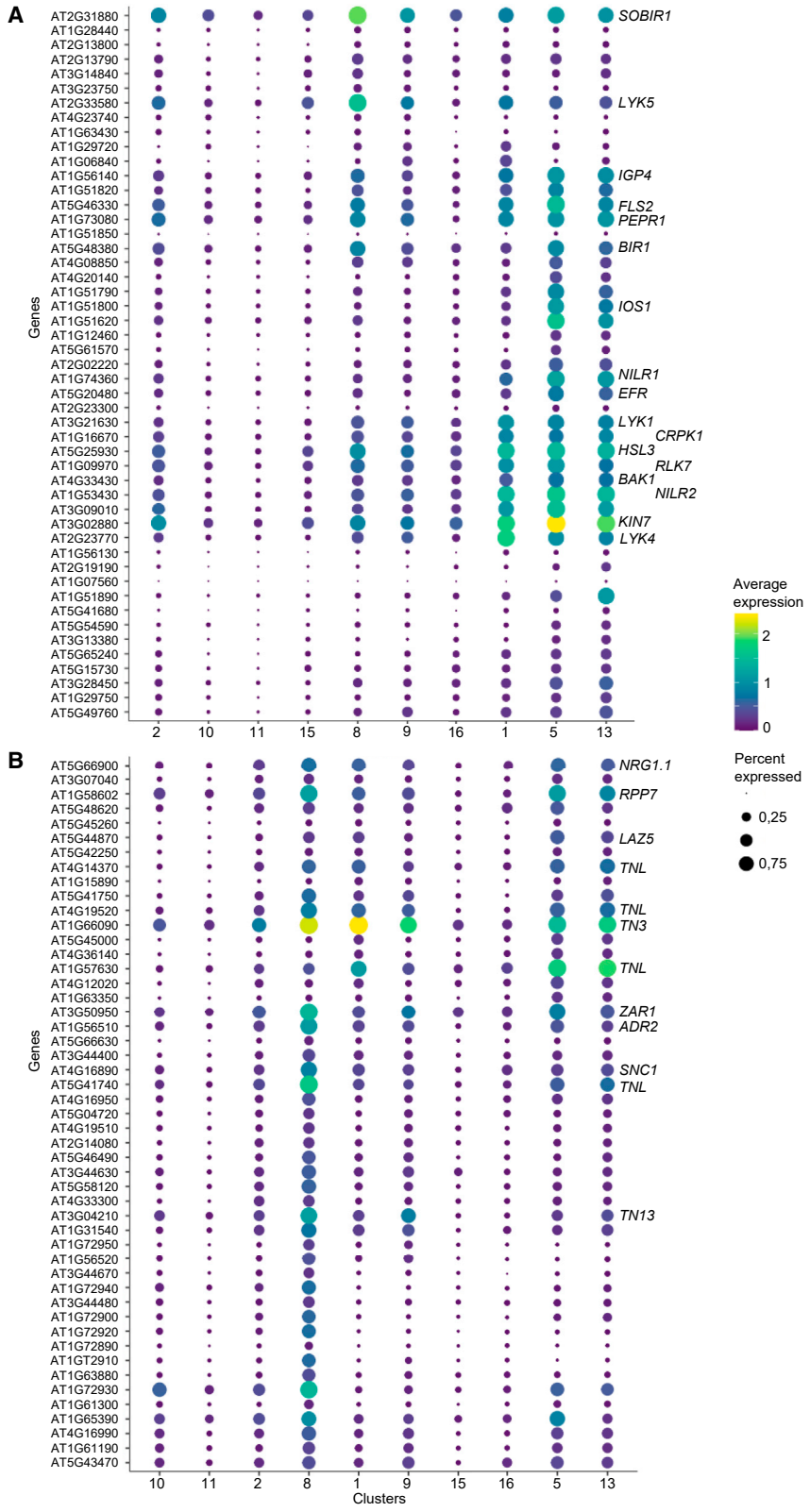

Figure 3. Cluster-specific expression profiles of immune receptor genes.

(A) Profiles for 49 selected *PRR* genes. For profiles of the total 236 *PRR* genes, see Supplemental Figure 5.

(B) Profiles for 59 selected *NLR* genes. For profiles of the total 207 *NLR* genes, see Supplemental Figure 6. Some common gene symbols are given on the right of the figure.

populations, in contrast, the NLRs are the most numerous to be strongly expressed in the responsive mesophyll cells (C8). This actually could indicate that the two cell types promote different immunities in response to *Pst*, and that epidermal cells are more proficient in PTI, whereas mesophyll cells are more proficient in ETI.

Convergence and divergence of cell-type responses to *Pst*

To investigate the dynamics of single-cell responses to *Pst*, we processed our clustering data with Monocle3. This allows the creation of cell trajectories which correspond to characteristic paths linking different cell fates or transcriptomic states through progressive transcriptional changes found in several different cells. Monocle3 also generates modules that group together genes showing identical expression dynamics along the trajectory within a single cluster or between several clusters. As shown in Figure 4A, Monocle3 built three cell trajectories from our clustering data. The first one in the C16 guard cell populations is linear and links two distinct cell fates. The second one is in the C15 companion cells with a branching point and three distinct cell fates. The last one links the C2 vascular S cells, the C1 and C9 epidermal cells, the C10, C11, and C8 mesophyll cells as well as the C5 and C13 cells with ten branching points and ten distinct cell fates. Interestingly it appears that C5 and C13 correspond to a single cell fate (cell fate 10) toward which all vascular S cells, epidermal cells, and mesophyll cells could converge, suggesting that these cell types could dedifferentiate in response to *Pst* and acquire new defense functions through a common and shared reprogramming. It also appears that the three cell types can diverge along a second trajectory path, at the branching point 6 for epidermal cells, 10 for vascular S cells and 8 for mesophyll cells, leading to cell-type-specific responses.

To get an insight into the transcriptional processes that could drive the convergence of mesophyll, epidermal, and vascular S cells, we identified 13 gene modules among the 71 generated by Monocle3 (see Additional Supplemental File) that display high expression scores around cell fate 10 in the clusters C5 and C13, and low expression scores in healthy mesophyll cells, healthy epidermal cells and

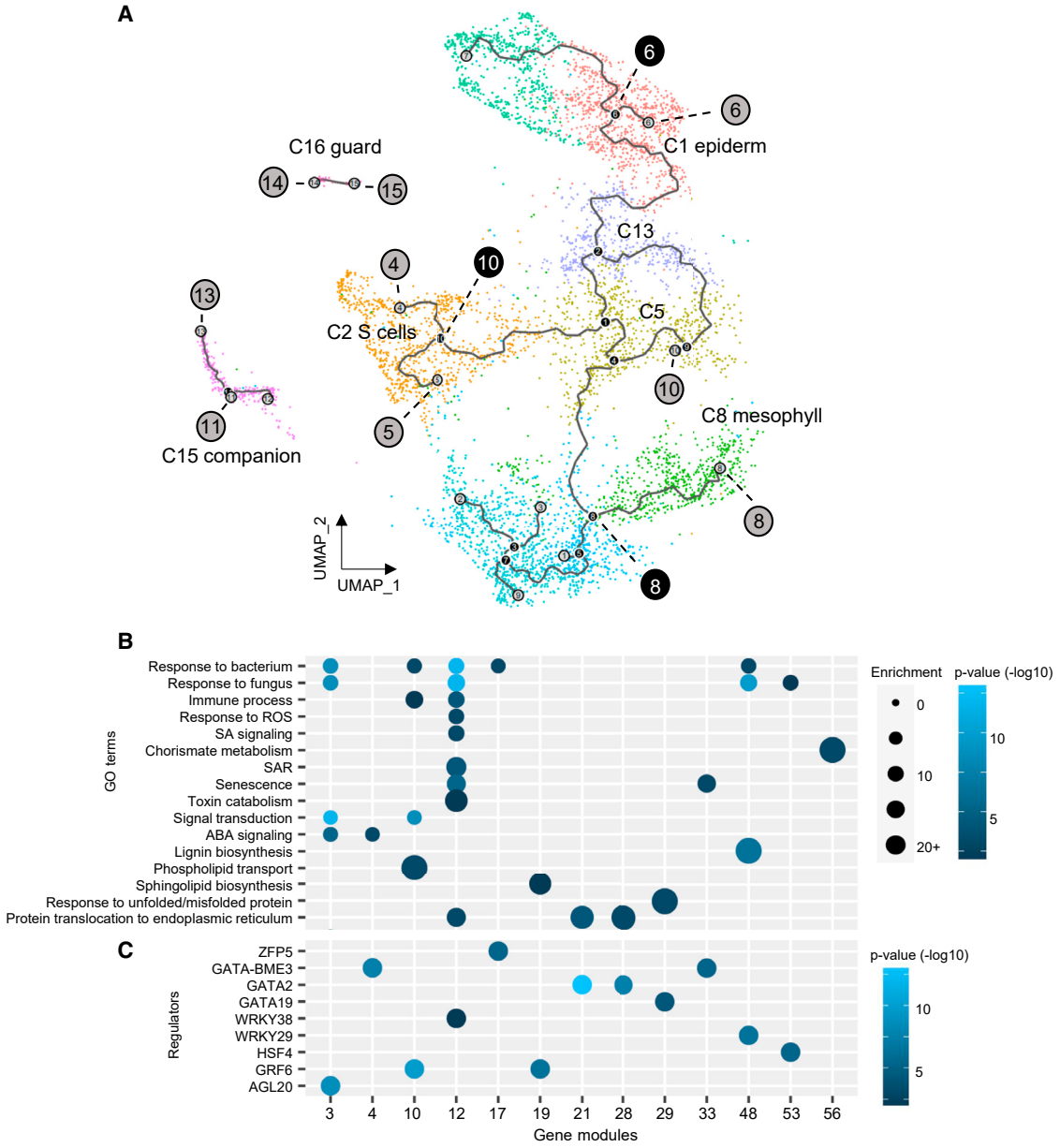

Figure 4. Convergence and divergence of cell responses to *Pst*.

(A) Cell trajectories were built using Monocle3 (see methods) and the UMAP projection of Figure 1E. Black circles indicate branching points. Gray circles indicate cell fates.

(B) Enrichments in biological processes for genes in selected modules. The enrichments and associated p values were generated using Panther. For a complete list of GO enrichments, see Supplemental Table 5.

(C) List of regulators for genes in each module. The list and p values were generated using TF2Network. Only the first-ranked regulator for each module is shown. For a complete list of regulators, see Supplemental Table 6.

vascular S cells. Those modules 3, 4, 10, 12, 17, 19, 21, 28, 29, 33, 48, 53, and 56 show strong enrichments in detoxification, lignification, defense responses to biotic stress, sphingolipid metabolism, vacuolar transport, protein targeting to the endoplasmic reticulum, senescence, and chorismate metabolism (Figure 4B), suggesting that these processes are important to mediate the responsive cell convergence toward cell fate 10. Moreover, as chorismate is the precursor of SA, we wondered whether SA synthesis could have a role in the convergence of the different cell types. To answer this question, we looked at the expression profiles of several genes involved in SA synthesis and signaling. If the results for *SARD1*, *CBP60g*, and *PR5* are not really conclusive, the expression patterns of *ICS1*, *PBS3*, *PR1*, and *PR2* are indeed compatible with the notion that activation of SA synthesis and signaling are characteristic of responses converging toward cell fate 10 (Supplemental Figure 7). Even more interestingly we noticed that transcriptional reprograming of the 13 modules are predominantly governed by WRKY transcription factors as well as by regulators known to be

involved in plant development, including several GATA transcription factors (Figure 4C), possibly uncovering a new function for these proteins in mediating cell convergence and dedifferentiation during defense responses.

New functions and transcriptional dynamics of cell-type-specific responses to *Pst*

We further analyzed the gene modules generated by Monocle3 to characterize the cell-type-specific responses to *Pst*. For instance, in the companion cells, modules 1, 15, 20, and 58 coincide with cell fate 13 while cell fate 11 coincides with module 23 (Figure 5A). As modules 1, 20, and 58 show enrichments in defense responses to bacterium or SA signaling and are mostly regulated by CAMTA transcription factors (Figures 5D and 5E), we inferred that cell fate 13 corresponds to the responsive companion cells, whereas cell fate 11, characterized by polyamine synthesis (Figure 5D) should be associated with healthy companion cells. Interestingly module 15 shows important enrichment in calcium transport (Figures 5A and 5D), hinting at a possible role for companion cells in calcium signaling and transport during defense responses to *Pst*. Similarly, modules 1, 3, 4, 33, and 53, enriched in immune processes and SA signaling, show strong expression scores in the guard cells located around cell fate 15 (Figures 5B and 5D), indicating that those might correspond to the ones that are the most responsive to *Pst*. Besides, we found that module 69 is also specific to cell fate 15 (Figure 5B). Although this module does not show any peculiar GO enrichment, it includes several genes involved in ABA signaling such as the receptor *PYL2* and the anion channel *SLAC1* (Supplemental Table 5), reinforcing our interpretation that guard cells mostly respond to *Pst* in an ABA-dependent manner. In contrast modules 13, 26, and 49, enriched in genes related to translation (Figure 5D), show high expression scores toward cell fate 14 (Figure 5B) corresponding to healthy guard cells, thereby illustrating how translation processes are repressed in response to *Pst* in this cell type. Concerning the vascular C2 cells, we found that modules 46 and 66, enriched in processes related to vasculature development, were highly expressed around cell fate 4, while module 42, enriched in glucosinolate synthesis, callose deposition, and that is mainly governed by MYB transcription factors, is highly expressed around cell fate 5 (Figures 5C–5E). These observations are compatible with our interpretation that S cells correspond to a cell type specifically induced in response to *Pst*.

For the epidermal and mesophyll cells, by comparing the different modules that characterize them, with the pseudotime values of each cell (Supplemental Figures 8A, 8B, 9A, and 9B), we could reconstruct the transcriptional dynamics of their respective responses to *Pst*, unveiling the genes as well as the biological processes that are repressed or induced in an early, late, or transient manner, and highlighting the main regulators responsible for these evolutions (Supplemental Figures 8C–8E and 9C–9E). This approach notably confirmed that Et signaling is rapidly repressed after induction in epidermal cells (Supplemental Figure 8).

Taken collectively, our analysis with Monocle3 allowed us to further refine our understanding of responses to *Pst*, raising several new hypotheses regarding the specialization of the different cell types in response to the pathogen.

Identification of common responses to *Pst* between different cell types characterized by SA/JA-ABA antagonism

Analysis of the gene modules generated by Monocle3 also allowed the identification of the modules 1, 5, 7, 14, 20, 43, and 58 as having strong expression scores in different responsive cells (Figure 6A). This indicates that they very likely represent general stress reprogramming that can be shared between different cell types, a possibility that has also been advanced in another recent study (Nobori et al., 2023). Remarkably, these modules show strong enrichments in different processes related to biotic stress responses, including SA, JA, and ABA signaling (Figure 6B). We also found that modules 5 and 43 are mostly governed by transcription factors involved in ABA and JA signaling, such as ABI5, ABF1, ABF4, PIF1, and MYC3, while other modules are regulated mainly by CAMTA1/2/3 which are key actors in the activation of SA signaling (Figure 6C). Altogether these data show that, in response to *Pst*, different cell types can undergo common gene reprogramming that are characterized by an SA/JA-ABA antagonism. Hence, these data support the notion that susceptible and immune processes could operate simultaneously in all the responsive cell types. In line with this, the expression profiles of ABA synthesis and signaling genes globally indicate that ABA-related processes are ubiquitous in our clustering (Supplemental Figure 10A). We also looked at the transcript levels of 28 genes that are presented as markers of susceptibility (Zhu et al., 2022), but, as shown in Supplemental Figure 10B, no clear pattern could be deduced from our data, several of the genes being expressed in numerous cells and at high levels in various populations, regardless of the identities or the nature (healthy/responsive) of these latter.

DISCUSSION

In this scRNA-seq study, although we worked with protoplasts and did not include mock conditions, we were able to decipher the plant defense response to a pathogen at an unprecedented single-cell resolution. Importantly, our data are not only consistent with the current knowledge on the topic, but they also raise several new interesting hypotheses regarding the *Arabidopsis*/*Pseudomonas* interactions, and provide a wealth of information for further molecular investigations. An attempt to integrate all this is presented in Figure 7. In the following, we discuss briefly how our data bring original elements to three fundamental questions.

Are all cell types immune totipotent?

On the basis of the list of marker genes in the Seurat clustering as well as on the gene modules of Monocle3, we could identify and characterize cell-type defense responses, showing that all cell types do not respond identically to the pathogen and that they can specialize in peculiar defense processes. Remarkably we could associate the distinct transcriptional reprogramming with specific sets of regulators, indicating that transcription factors known to be involved in the response to *Pst* (e.g., WRKYs, CAMTAs, MYBs, ANACs) may act prominently in

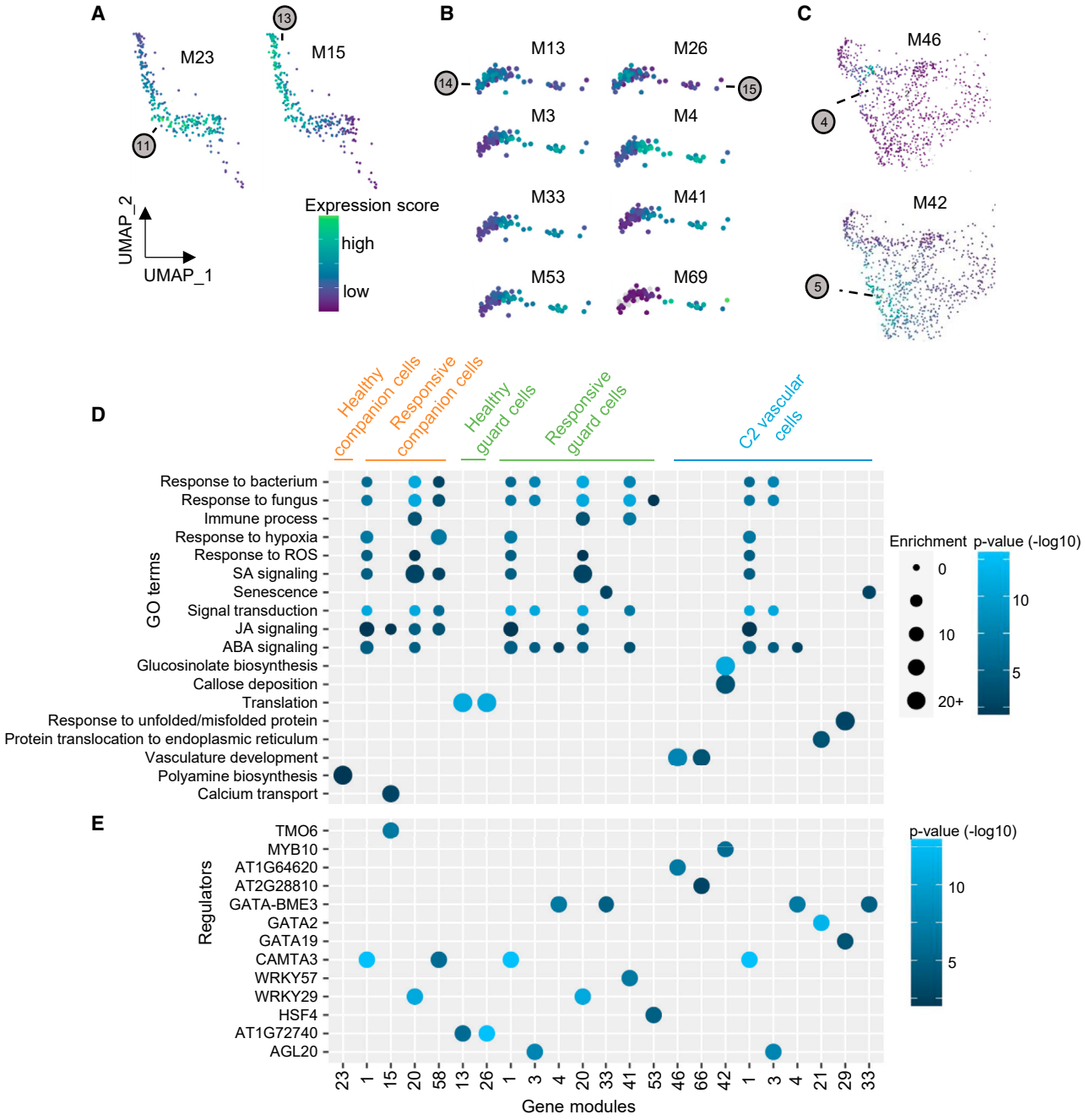

Figure 5. Transcriptional dynamics of responses to *Pst* in companion, guard, and vascular cells.

(A–C) Examples of gene modules showing high expression scores around different cell fates in companion cells **(A)**, in guard cells **(B)**, and in vascular cells **(C)**. For complete, high-resolution pictures and precise values of expression scores, see Additional Supplemental File. The cell fates are indicated in gray circles (see Figure 4).

(D) Enrichments in biological processes for selected gene modules corresponding to responsive and non-responsive populations. The enrichments and the associated p values were generated using Panther. For a complete list of GO enrichments, see Supplemental Table 5.

(E) List of regulators for selected gene modules. The list and p values were generated using TF2Network. Only the first-ranked regulators are shown. For a complete list of regulators, see Supplemental Table 6.

selective cell populations. Similarly, we found that the expression profiles of key immune receptors can vary considerably between different cell clusters, suggesting that all cell types are not equal in their ability to sense the pathogen, and that some might be more proficient than others in specific kinds of immunity. In this regard, it could be interesting to reexamine the crosstalk between PTI and ETI as hinging not on intracellular but rather on intercellular mechanisms. Parallel to this, we observed that the different cell types can also undergo common modules of transcriptional reprogramming mediated

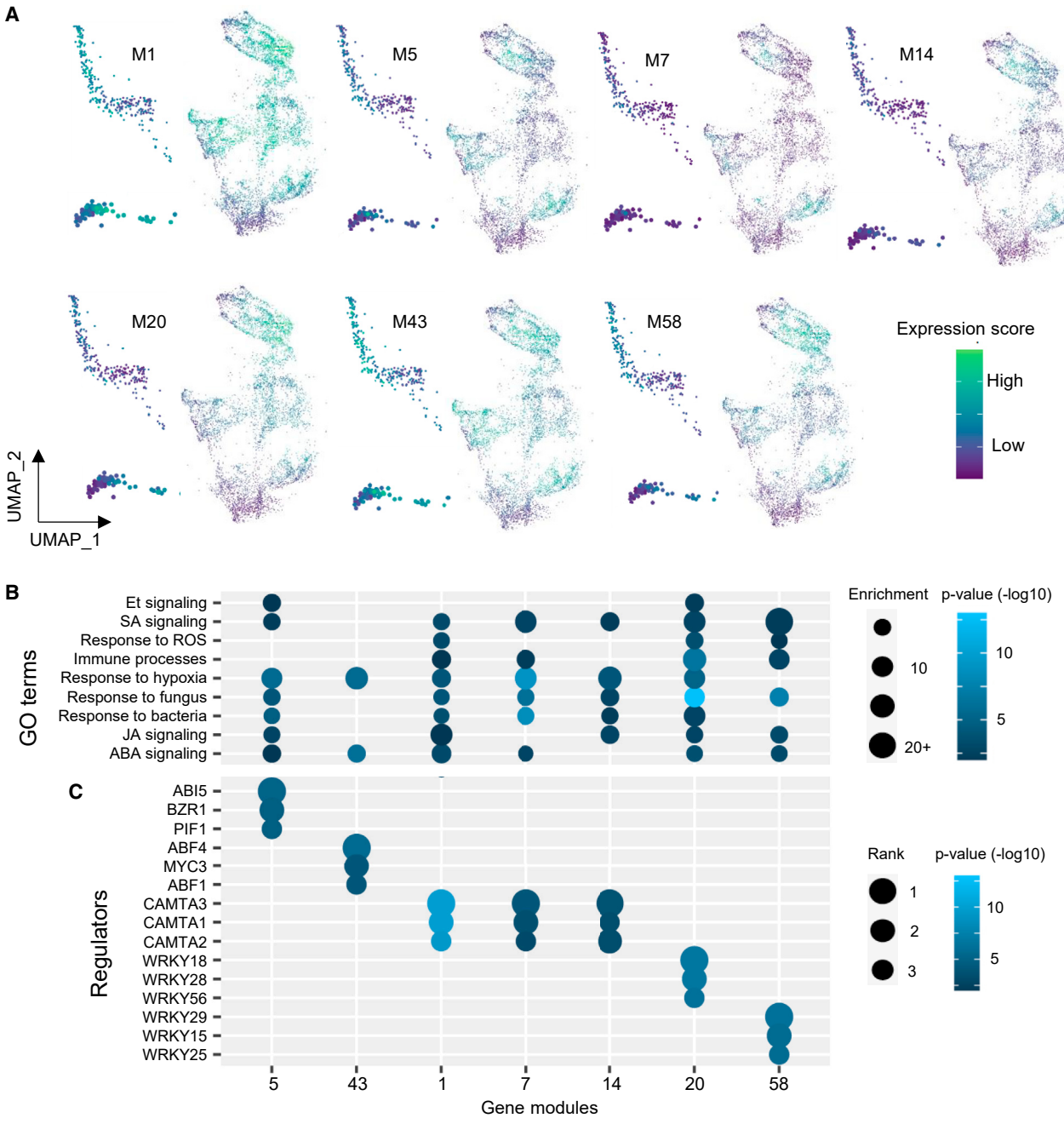

Figure 6. Characterization of transcriptional responses to *Pst* common to different cell types.

(A) Selected modules showing high expression scores in different cell types. For complete, high-resolution pictures and precise values of expression scores, see Additional Supplemental File.

(B) Enrichments in biological processes for selected gene modules. The enrichments and associated p values were generated using Panther. For a complete list of GO enrichments, see Supplemental Table 5.

(C) List of regulators for selected gene modules. The list, the ranks, and the p values were generated using TF2Network. Only the three first-ranked regulators for each module are shown. For a complete list of regulators, see Supplemental Table 6.

by shared regulators. The construction of cell trajectories even supports the possibility that, in response to *Pst*, epidermal, mesophyll, and some vascular cells can converge toward a unique cell fate characterized mainly by resistance functions such as lignification, detoxification, or phytoalexin synthesis, and for which GATA transcription factors might play an important role.

From this, emerges a scenario where the defense responses of the different cell types (at least for mesophyll, vascular S, and epidermal cells) could be divided into two components. The first one would be shared and resistance centered and could therefore substantiate the notion of immune totipotency. The second one would be cell type specific, and would allow the implementation and coordination of several distinct protective measures. If

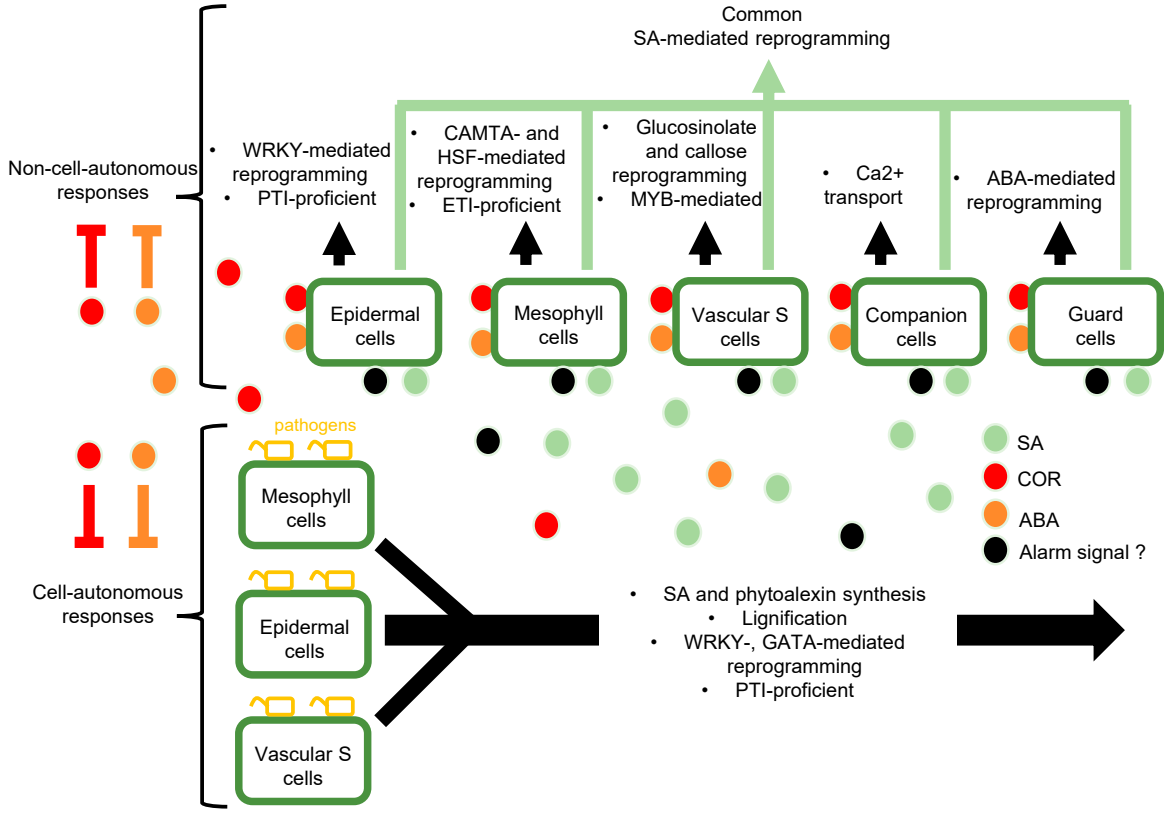

Figure 7. Model of transcriptional defense reprogramming at the cell-type level in response to *Pst*.
In the first step, pathogen detection triggers cell-autonomous responses (lower part), mediated by immune totipotency and resulting in the synthesis of signal alarms such as SA, as well as in the synthesis of phytoalexins and lignin acting as barriers against the pathogen. These cell-autonomous responses concern mostly the epidermal cells that are the first ones to encounter the pathogens and where the expression levels of the immune receptors are the highest. In a second step, alarm signals trigger non-cell-autonomous responses (upper part). Features of the cell-type specific non-autonomous responses are indicated by black arrows. The common component of non-cell-autonomous responses, mostly mediated by SA signaling is indicated by a green arrow. Concomitantly coronatine produced by *Pst* and ABA antagonize autonomous and non-autonomous responses, limiting cell evolutions toward immune populations.

so, the factors that determine the respective influence of these two response components still need to be elucidated.

How do susceptibility and immunity take place at the single cell level?

In a recent scRNA-seq study, it was proposed that, upon *Pst* infection, cells would evolve from early immune responses to late susceptible responses (Zhu et al., 2022). Our own data do not really retrieve this pattern, showing rather a concurrent activation of immune and susceptible processes in all the cells. A simple explanation for this discrepancy could be differences in the experimental set up between the two studies. Indeed, we performed our analyses earlier than in Zhu et al. (2022) (16 vs. 24 hpi), it is therefore possible that our data lack the strong and late susceptible responses. An alternative could be differences in the degree of plant resistance or pathogen virulence between the two experiments. Our interpretation is that immune and susceptible processes occur synchronously in all cells, and that it is this competition that drives cell evolution toward specific responsive populations. In this regard, the outcome of a pathogen infection might be more reliably predicted by the relative sizes or proportions of these responsive populations rather than by the expression features of some susceptible or immune genes. According to this, the absence in Zhu et al. (2022) of clusters equivalent to C5 and C13 could indicate that the plants of this study are more susceptible than ours. In the future it would be greatly interesting to test the hypothesis mentioned above, with scRNA-seq analyses of leaves inoculated with different strains of *Pst* that are more or less virulent.

What are the cell-autonomous and non-cell-autonomous responses to *Pst*?

To explain the divergence of the mesophyll, epidermal, and vascular S cells into two separate populations, an exciting possibility could be that it reflects the difference between cell-autonomous and non-cell-autonomous responses. In this case, we would have on one hand the C13 and C5 populations, composed of cells coming from different types, not only committed to stop the pathogens, but also essential for the synthesis of proximal or distal alarm signals, such as SA. This would correspond to the autonomous responses of cells directly in contact with the pathogens (i.e., at the closest of the battle-fronts) and characterized by the immune-totipotent component of the defense responses. On the other hand, we would have cell-type-characteristic responses, triggered by intercellular

communication, and allowing plant cells to mount prophylactic measures in anticipation of upcoming pathogen attacks. This would correspond to the non-cell-autonomous responses, mediated by both common and specific components of the defense transcriptional reprogramming. If such a model is true, the nature of the intercellular signals as well as the efficiency of the cell-type-specific responses to impede infection remain to be clarified. Furthermore, this model could help explain the colonization strategy of *Pst*. Indeed, cell-autonomous responses characterized by strong PTI are predominant in epidermal cells that are the first plant cells to face the pathogens. This would stimulate the bacteria to move toward cell types, such as guard, vascular, or mesophyll cells, where autonomous responses are milder because of lower levels of *PRR* expression, and where the pathogen would mostly compete with non-cell-autonomous responses, leading ultimately to more or less virulent proliferation.

METHODS

Plant materials and growth conditions

Plants from this study are in the Columbia background. They were grown in soil, in growth chambers at 20°C, in short day conditions (8 h light, from 9 am to 5 pm), at 60% hygrometry and under a light intensity of approximately 150 μmol m^{-2} s^{-1}.

Bacterial infections

Bacterial infections were performed on 6-week-old plants by spraying. The *Pst* wild-type (WT) strain was grown on LB medium supplemented with 50 μg/mL rifampicin. Fresh cultures in mid-exponential phase were washed, resuspended in 10 mM $MgCl_2$ at a final optical density at 600 nm (OD_{600}) of 0.1, and supplemented with 0.04% of Silwet L-77. For the three independent replicates, spraying took place at the end of the day (between 5:30 pm and 6 pm), and leaves were collected 16 h later (between 9:30 am and 10 am). During this period, plants remained uncovered.

Protoplast preparation, and scRNA-seq library preparation and sequencing

For each biological replicate, about 20–25 leaves coming from 8 independent plants were cut in thin slices with a razor blade, and digested in an enzymatic solution (1.5% Cellulase R10, Yakult, 0.4% Macerozyme R-10, Yakult, 400 mM Mannitol, 20 mM KCl, 20 mM MES [pH 5.7], 10 mM $CaCl_2$, and 0.1% BSA), under vacuum at room temperature (RT) for 15 min, and then in growth chamber (20°C) for 50 min. The protoplast solutions were filtered through a 70 μm mesh and a 40 μm cell strainer, with mild centrifugation (1 min, 150 g), and resuspended each time in W5 buffer (150 mM NaCl, 125 mM $CaCl_2$, 5 mM KCl, and 2 mM MES [pH 5.7]). After concentration measurements using a hemocytometer, protoplasts were recovered by centrifugation and resuspended in PBS buffer supplemented with 0.04% of BSA at a final concentration of 1000 cells/μL. Eight thousand protoplasts were then processed using the Next GEM Single Cell 3′ library kit version 3.1 (10X Genomics) following the supplier's instructions, and the libraries were sequenced on an Illumina NextSeq500 at the POPS platform (https://ips2.u-psud.fr/en/platforms/spomics-interactomics-metabolomics-transcriptomics/pops-transcriptomic-platform.html.)

scRNA-seq data processing

For each biological replicate, sequencing data were preprocessed with Cell Ranger (version 4.0.0; 10X Genomics) using default parameters and the Araport11 as *Arabidopsis* reference genome. The preprocessed data were pooled by concatenation and analyzed with the Seurat R package (version 3.2.2) (Stuart et al., 2019). Genes expressed in 3 cells or less as well as cells expressing 200 genes or less were removed from the analysis. The tolerated percentages of mitochondrial and chloroplastic reads per cell were set at 5%. Cells were normalized via the SCTransform function and principal-component analysis (PCA) was performed on the 2000 most variable features using the FindVariableFeatures function where 30 dimensions were kept. We clustered the cells with the FindClusters function, using the Louvain algorithm and a resolution r = 1. The neighbors used to perform the clustering algorithm were found using the FindNeighbors function. A Wilcoxon rank-sum test has been performed to identify the marker genes, using the FindAllMarkers function with min.pct and logfc.threshold parameters set at 0.25.The Monocle3 package (version 1.0.0) (Cao et al., 2019) (https://cole-trapnell-lab.github.io/monocle3/) was used for analysis of transcriptional dynamics. Seurat object was transferred into a Monocle3 cell_data_set object using SeuratWrappers (version 0.3.1) (https://github.com/satijalab/seurat-wrappers). The cluster_cells function was used to compute partitions needed for trajectory analysis and then clusters were reassigned to previously computed clusters found with Seurat. Cell trajectories were built using the learn_graph function. For pseudotime calculations, the order_cell function was used and the root nodes were chosen manually for each cell type. We measured the multi-directional and multi-dimensional spatial autocorrelation using the Moran's 1 measure, implemented in the graph_test function. Only genes with high confidence (q < 5.10–10) on the Moran's I test were retained to form the gene modules. Gene modules were obtained using the find_gene_modules function with a resolution r = 0.01.

For visualization, the gene expression space was reduced using UMAP. The expression profiles of individual genes and the pseudotime values in each cell were obtained using the plot_cell function (Monocle3). The expression profiles of individual genes in clusters were obtained using the plot_gene_by_group function (Monocle3). The expression scores of gene modules, in cells and in clusters, were obtained using the plot_cell function and the aggregate_gene_expression function (Monocle3).

DATA AND CODE AVAILABILITY

The scRNA-seq data from this study are deposited in the NCBI Bioproject PRJNA995336 (https://www.ncbi.nlm.nih.gov/bioproject/PRJNA995336) and the outputs from Cell Ranger in the INRAE Dataverse (https://doi.org/10.57745/CKVGIN). The code used to analyze the data is available at https://github.com/Bastien-mva/pipeline_seurat_monocle.

SUPPLEMENTAL INFORMATION

Supplemental information is available at *Plant Communications Online*.

FUNDING

This study was supported by INRAE funding (SCANNER project, BAP Department). The POPS platform benefits from the support of Saclay Plant Sciences-SPS (ANR-17-EUR-0007).

AUTHOR CONTRIBUTIONS

Conceptualization, J.L.; Methodology, E.D. and J.L.; Software, B.B.; Investigation, E.D., S.P., L.S.-T., and J.L.; Data Curation, E.D. and B.B.; Original Draft, J.L.; Review & Editing, E.D., B.B., J. Chiquet, J. Colcombet, and J.L.; Visualization, J.L.; Supervision, J. Chiquet and J. Colcombet; Project Administration, E.D. and J.L.; Funding Acquisition, J.L.

ACKNOWLEDGMENTS

The authors thank the IPS2 bioinformatic platform (Marion Verdenaud and Frédéric Desprez, https://ips2.u-psud.fr/en/presentation/services-d-appui-a-la-recherche/bioinformatic-tray.html) for facilitating installations of the Seurat and Monocle3 packages. The authors also thank Marie Boudsocq (Researcher, CNRS) for technical assistance with protoplast preparation. No conflict of interest is declared.

Received: May 15, 2023
Revised: July 24, 2023
Accepted: August 24, 2023
Published: August 28, 2023

REFERENCES

Barth, C., and Jander, G. (2006). Arabidopsis myrosinases TGG1 and TGG2 have redundant function in glucosinolate breakdown and insect defense. Plant J. **46**:549–562.

Bharath, P., Gahir, S., and Raghavendra, A.S. (2021). Abscisic Acid-Induced Stomatal Closure: An Important Component of Plant Defense Against Abiotic and Biotic Stress. Front. Plant Sci. **12**, 615114.

Cao, J., Spielmann, M., Qiu, X., Huang, X., Ibrahim, D.M., Hill, A.J., Zhang, F., Mundlos, S., Christiansen, L., Steemers, F.J., et al. (2019). The single-cell transcriptional landscape of mammalian organogenesis. Nature **566**:496–502.

de Torres-Zabala, M., Truman, W., Bennett, M.H., Lafforgue, G., Mansfield, J.W., Rodriguez Egea, P., Bögre, L., and Grant, M. (2007). Pseudomonas syringae pv. tomato hijacks the Arabidopsis abscisic acid signalling pathway to cause disease. EMBO J. **26**:1434–1443.

Dhar, N., Caruana, J., Erdem, I., and Raina, R. (2020). An Arabidopsis DISEASE RELATED NONSPECIFIC LIPID TRANSFER PROTEIN 1 is required for resistance against various phytopathogens and tolerance to salt stress. Gene **753**, 144802.

Emonet, A., Zhou, F., Vacheron, J., Heiman, C.M., Dénervaud Tendon, V., Ma, K.-W., Schulze-Lefert, P., Keel, C., and Geldner, N. (2021). Spatially Restricted Immune Responses Are Required for Maintaining Root Meristematic Activity upon Detection of Bacteria. Curr. Biol. **31**:1012–1028.e7.

Fan, J., Crooks, C., Creissen, G., Hill, L., Fairhurst, S., Doerner, P., and Lamb, C. (2011). *Pseudomonas sax* Genes Overcome Aliphatic Isothiocyanate-Mediated Non-Host Resistance in *Arabidopsis*. Science **331**:1185–1188.

Flors, V., Ton, J., van Doorn, R., Jakab, G., García-Agustín, P., and Mauch-Mani, B. (2008). Interplay between JA, SA and ABA signalling during basal and induced resistance against Pseudomonas syringae and Alternaria brassicicola. Plant J. **54**:81–92.

Friedman, R., Levin, N., and Altman, A. (1986). Presence and identification of polyamines in xylem and Phloem exudates of plants. Plant Physiol. **82**:1154–1157.

Geng, X., Cheng, J., Gangadharan, A., and Mackey, D. (2012). The coronatine toxin of Pseudomonas syringae is a multifunctional suppressor of Arabidopsis defense. Plant Cell **24**:4763–4774.

Hou, S., Wang, X., Chen, D., Yang, X., Wang, M., Turrà, D., Di Pietro, A., and Zhang, W. (2014). The secreted peptide PIP1 amplifies immunity through receptor-like kinase 7. PLoS Pathog. **10**, e1004331.

Hsu, F.-C., Chou, M.-Y., Chou, S.-J., Li, Y.-R., Peng, H.-P., and Shih, M.-C. (2013). Submergence confers immunity mediated by the WRKY22 transcription factor in Arabidopsis. Plant Cell **25**:2699–2713.

Hu, Y., Ding, Y., Cai, B., Qin, X., Wu, J., Yuan, M., Wan, S., Zhao, Y., and Xin, X.-F. (2022). Bacterial effectors manipulate plant abscisic acid signaling for creation of an aqueous apoplast. Cell Host Microbe **30**:518–529.e6.

Jelenska, J., van Hal, J.A., and Greenberg, J.T. (2010). Pseudomonas syringae hijacks plant stress chaperone machinery for virulence. Proc. Natl. Acad. Sci. USA **107**:13177–13182.

Jiménez-Bremont, J.F., Marina, M., Guerrero-González, M.d.l.L., Rossi, F.R., Sánchez-Rangel, D., Rodríguez-Kessler, M., Ruiz, O.A., and Gárriz, A. (2014). Physiological and molecular implications of plant polyamine metabolism during biotic interactions. Front. Plant Sci. **5**:95.

Jones, J.D.G., and Dangl, J.L. (2006). The Plant Immune System. Nature **444**:323–329.

Jones, J.D.G., Vance, R.E., and Dangl, J.L. (2016). Intracellular innate immune surveillance devices in plants and animals. Science **354**:aaf6395.

Kim, J.-Y., Symeonidi, E., Pang, T.Y., Denyer, T., Weidauer, D., Bezrutczyk, M., Miras, M., Zöllner, N., Hartwig, T., Wudick, M.M., et al. (2021). Distinct identities of leaf phloem cells revealed by single cell transcriptomics. Plant Cell **33**:511–530.

Kulkarni, S.R., Vaneechoutte, D., Van de Velde, J., and Vandepoele, K. (2018). TF2Network: predicting transcription factor regulators and gene regulatory networks in Arabidopsis using publicly available binding site information. Nucleic Acids Res. **46**:e31.

Lang, J., Genot, B., Bigeard, J., and Colcombet, J. (2022). MPK3 and MPK6 control salicylic acid signaling by up-regulating NLR receptors during pattern- and effector-triggered immunity. J. Exp. Bot. **73**:2190–2205.

Lee, M.-H., Jeon, H.S., Kim, S.H., Chung, J.H., Roppolo, D., Lee, H.-J., Cho, H.J., Tobimatsu, Y., Ralph, J., and Park, O.K. (2019). Lignin-based barrier restricts pathogens to the infection site and confers resistance in plants. EMBO J. **38**, e101948.

Lewis, L.A., Polanski, K., de Torres-Zabala, M., Jayaraman, S., Bowden, L., Moore, J., Penfold, C.A., Jenkins, D.J., Hill, C., Baxter, L., et al. (2015). Transcriptional dynamics driving MAMP-triggered immunity and pathogen effector-mediated immunosuppression in Arabidopsis leaves following infection with Pseudomonas syringae pv tomato DC3000. Plant Cell **27**:3038–3064.

Lu, Y., and Tsuda, K. (2020). Intimate Association of PRR- and NLR-Mediated Signaling in Plant Immunity. Mol. Plant Microbe Interact. **34**:3–14.

Melotto, M., Zhang, L., Oblessuc, P.R., and He, S.Y. (2017). Stomatal Defense a Decade Later. Plant Physiol. **174**:561–571.

Meyers, B.C., Kozik, A., Griego, A., Kuang, H., and Michelmore, R.W. (2003). Genome-wide analysis of NBS-LRR-encoding genes in Arabidopsis. Plant Cell **15**:809–834.

Mine, A., Seyfferth, C., Kracher, B., Berens, M.L., Becker, D., and Tsuda, K. (2018). The defense phytohormone signaling network enables rapid, high-amplitude transcriptional reprogramming during effector-triggered immunity[OPEN]. Plant Cell **30**:1199–1219.

Nekrasov, V., Li, J., Batoux, M., Roux, M., Chu, Z.-H., Lacombe, S., Rougon, A., Bittel, P., Kiss-Papp, M., Chinchilla, D., et al. (2009). Control of the pattern-recognition receptor EFR by an ER protein complex in plant immunity. EMBO J. **28**:3428–3438.

Ngou, B.P.M., Ahn, H.-K., Ding, P., and Jones, J.D.G. (2021). Mutual potentiation of plant immunity by cell-surface and intracellular receptors. Nature **592**:110–115. https://doi.org/10.1038/s41586-021-03315-7.

Ngou, B.P.M., Ding, P., and Jones, J.D.G. (2022). Thirty years of resistance: Zig-zag through the plant immune system. Plant Cell **34**:1447–1478.

Nintemann, S.J., Hunziker, P., Andersen, T.G., Schulz, A., Burow, M., and Halkier, B.A. (2018). Localization of the glucosinolate biosynthetic enzymes reveals distinct spatial patterns for the biosynthesis of indole and aliphatic glucosinolates. Physiol. Plantarum **163**:138–154.

Nobori, T., Monell, A., Lee, T.A., Zhou, J., Nery, J., and Ecker, J.R. (2023). Time-resolved single-cell and spatial gene regulatory atlas of plants under pathogen attack. Preprint at bioRxiv. https://doi.org/10.1101/2023.04.10.536170.

Palm-Forster, M.A.T., Eschen-Lippold, L., Uhrig, J., Scheel, D., and Lee, J. (2017). A novel family of proline/serine-rich proteins, which are phospho-targets of stress-related mitogen-activated protein kinases, differentially regulates growth and pathogen defense in Arabidopsis thaliana. Plant Mol. Biol. **95**:123–140.

Qiu, J.-L., Fiil, B.K., Petersen, K., Nielsen, H.B., Botanga, C.J., Thorgrimsen, S., Palma, K., Suarez-Rodriguez, M.C., Sandbech-Clausen, S., Lichota, J., et al. (2008). Arabidopsis MAP kinase 4 regulates gene expression through transcription factor release in the nucleus. EMBO J. **27**:2214–2221.

Rich-Griffin, C., Stechemesser, A., Finch, J., Lucas, E., Ott, S., and Schäfer, P. (2020a). Single-Cell Transcriptomics: A High-Resolution Avenue for Plant Functional Genomics. Trends Plant Sci. **25**:186–197.

Rich-Griffin, C., Eichmann, R., Reitz, M.U., Hermann, S., Woolley-Allen, K., Brown, P.E., Wiwatdirekkul, K., Esteban, E., Pasha, A., Kogel, K.-H., et al. (2020b). Regulation of Cell Type-Specific Immunity Networks in Arabidopsis Roots. Plant Cell **32**:2742–2762.

Routaboul, J.-M., Bellenot, C., Clément, G., Citerne, S., Remblière, C., Charvin, M., Franke, L., Chiarenza, S., Vasselon, D., Jardinaud, M.-F., et al. (2022). Arabidopsis hydathodes are sites of intense auxin metabolism and nutrient scavenging. Preprint at bioRxiv. https://doi.org/10.1101/2022.12.01.518666.

Shiu, S.H., and Bleecker, A.B. (2001). Receptor-like kinases from Arabidopsis form a monophyletic gene family related to animal receptor kinases. Proc. Natl. Acad. Sci. USA **98**:10763–10768.

Shubchynskyy, V., Boniecka, J., Schweighofer, A., Simulis, J., Kvederaviciute, K., Stumpe, M., Mauch, F., Balazadeh, S., Mueller-Roeber, B., Boutrot, F., et al. (2017). Protein phosphatase AP2C1 negatively regulates basal resistance and defense responses to Pseudomonas syringae. J. Exp. Bot. **68**:1169–1183.

Stegmann, M., Monaghan, J., Smakowska-Luzan, E., Rovenich, H., Lehner, A., Holton, N., Belkhadir, Y., and Zipfel, C. (2017). The receptor kinase FER is a RALF-regulated scaffold controlling plant immune signaling. Science **355**:287–289.

Stuart, T., Butler, A., Hoffman, P., Hafemeister, C., Papalexi, E., Mauck, W.M., 3rd, Hao, Y., Stoeckius, M., Smibert, P., and Satija, R. (2019). Comprehensive Integration of Single-Cell Data. Cell **177**:1888–1902.e21.

Tenorio Berrío, R., Verstaen, K., Vandamme, N., Pevernagie, J., Achon, I., Van Duyse, J., Van Isterdael, G., Saeys, Y., De Veylder, L., Inzé, D., and Dubois, M. (2022). Single-cell transcriptomics sheds light on the identity and metabolism of developing leaf cells. Plant Physiol. **188**:898–918.

Toum, L., Torres, P.S., Gallego, S.M., Benavídes, M.P., Vojnov, A.A., and Gudesblat, G.E. (2016). Coronatine Inhibits Stomatal Closure through Guard Cell-Specific Inhibition of NADPH Oxidase-Dependent ROS Production. Front. Plant Sci. **7**:1851.

Velásquez, A.C., Oney, M., Huot, B., Xu, S., and He, S.Y. (2017). Diverse mechanisms of resistance to Pseudomonas syringae in a thousand natural accessions of Arabidopsis thaliana. New Phytol. **214**:1673–1687.

Xin, X.-F., Nomura, K., Aung, K., Velásquez, A.C., Yao, J., Boutrot, F., Chang, J.H., Zipfel, C., and He, S.Y. (2016). Bacteria establish an aqueous living space in plants crucial for virulence. Nature **539**:524–529.

Xin, X.-F., Kvitko, B., and He, S.Y. (2018). Pseudomonas syringae: what it takes to be a pathogen. Nat. Rev. Microbiol. **16**:316–328.

Xu, J., Li, Y., Wang, Y., Liu, H., Lei, L., Yang, H., Liu, G., and Ren, D. (2008). Activation of MAPK Kinase 9 Induces Ethylene and Camalexin Biosynthesis and Enhances Sensitivity to Salt Stress in Arabidopsis. J. Biol. Chem. **283**:26996–27006.

Yoo, S.-D., Cho, Y.-H., Tena, G., Xiong, Y., and Sheen, J. (2008). Dual control of nuclear EIN3 by bifurcate MAPK cascades in C2H4 signalling. Nature **451**:789–795.

Yu, A., Lepère, G., Jay, F., Wang, J., Bapaume, L., Wang, Y., Abraham, A.-L., Penterman, J., Fischer, R.L., Voinnet, O., and Navarro, L. (2013). Dynamics and biological relevance of DNA demethylation in Arabidopsis antibacterial defense. Proc. Natl. Acad. Sci. USA **110**:2389–2394.

Yuan, M., Jiang, Z., Bi, G., Nomura, K., Liu, M., Wang, Y., Cai, B., Zhou, J.-M., He, S.Y., and Xin, X.-F. (2021). Pattern-recognition receptors are required for NLR-mediated plant immunity. Nature **592**:105–109. https://doi.org/10.1038/s41586-021-03316-6.

Zhang, N., and Fan, Z. (2020). Transcriptional reprogramming during effector/flg22-triggered immune is independent of defense phytohormone signaling networks. Preprint at bioRxiv. https://doi.org/10.1101/2020.09.09.289629.

Zhang, W., Zhao, F., Jiang, L., Chen, C., Wu, L., and Liu, Z. (2018). Different Pathogen Defense Strategies in Arabidopsis: More than Pathogen Recognition. Cells **7**:252.

Zhang, K., Su, H., Zhou, J., Liang, W., Liu, D., and Li, J. (2019). Overexpressing the Myrosinase Gene TGG1 Enhances Stomatal Defense Against Pseudomonas syringae and Delays Flowering in Arabidopsis. Front. Plant Sci. **10**:1230.

Zhu, J., Lolle, S., Tang, A., Guel, B., Kvikto, B., Cole, B., and Coaker, G. (2022). Single-cell profiling of complex plant responses to Pseudomonas syringae infection. Preprint at bioRxiv. https://doi.org/10.1101/2022.10.07.511353.

Zipfel, C. (2014). Plant pattern-recognition receptors. Trends Immunol. **35**:345–351.